Reactivity and Anisotropic Interaction of 1,3,5-$C_6H_3F_3$ and C_6F_6 with He*(2^3S) Atoms: Comparison with Mono- and Di-fluorobenzenes

Kohei Imura, Naoki Kishimoto, and Koichi Ohno*

Department of Chemistry, Graduate School of Science, Tohoku University, Aramaki, Aoba-ku, Sendai 980-8578, Japan

Received: June 26, 2001; In Final Form: September 4, 2001

Two-dimensional (collision-energy/electron-energy-resolved) Penning ionization electron spectroscopy (2D-PIES) have been applied to the reaction of 1,3,5-$C_6H_3F_3$ and C_6F_6 with metastable He*(2^3S) atoms. Collision energy dependence of the partial ionization cross sections (CEDPICS), which reflects interaction potential energy between the molecule and the He*(2^3S) atom, indicated anisotropic interaction around the molecules. Assignments of the Penning ionization electron spectra and He I ultraviolet photoelectron spectra have been made by the characteristics of the 2D-PIES. Furthermore, substituent effects on the reactivity of molecular orbitals and also on the interactions around the molecules for various fluorobenzenes were investigated. It was found that the reactivity of the molecular orbitals were closely related to the amount of F atomic orbital components in the orbital. Furthermore, an elucidation of the substituent effect on the interaction behaviors around the molecules gives us important insights on the dynamics of the colliding particles.

I. Introduction

The Penning ionization[1] of several molecules with metastable He* atoms has been widely investigated.[2] Throughout these studies, it has been well-recognized that the He* atom can be regarded as the simplest electrophilic reagent because the He* atom extracts an electron from a molecular orbital (MO) of the molecules. The Penning ionization process can be explained by the electron exchange model, in which an electron of the target MO is transferred into the inner vacant 1s orbital of the He* atom, which subsequently ejects the external electron in 2s orbital.[3] Therefore, the mutual overlap of related orbitals for the electron exchange plays a central role.[4,5] Penning ionization electron kinetic energy spectrum (PIES) provides us information on the electron distribution of the target MOs exposed outside the boundary surface of collision. It has been suggested that anisotropic interaction around the molecule also influences the dynamics of Penning ionization reaction.[6−9] Electron kinetic energy (E_e) and collision-energy (E_c) resolved two-dimensional (2D) PIES[6] have been used to investigate not only the orbital reactivity, but also the dynamics of the particles on the anisotropic interaction potential energy surface. This technique has recently been developed in our laboratory[6] and makes it possible to study the collision energy dependence of the partial ionization cross sections (CEDPICS) and collision-energy-resolved PIES (CERPIES). Thus, the state-resolved measurement of partial cross sections for the various ionic states enable us to investigate anisotropic potential surface around the target molecule.

Anisotropic interaction around the halogen atoms with metastable atoms[7−10] has been discussed by investigating the collision energy dependence of the Penning ionization reaction. Tokue et al.[7] reported that perpendicular approaches of the He*-(2^3S) atoms with respect to C−Cl bond axis was attractive in He*-CH_3Cl interacting system, while Alberti et al.[8] suggested that the attractive interaction was localized around the angle of 45° with respect to the C−Cl bond axis in Ne*($^3P_{2,0}$)-CH_3Cl system. These results are quite interesting because both results indicate that the location of the attractive interaction does not simply correlate with the local dipole direction (C−Cl bond axis). Yamato et al.[9] have studied the reaction of Ar*($^3P_{2,0}$) with $CHCl_3$ by using a combination of a time-of-flight techniques and an electric hexapole orientation technique and discussed the correlation between collision energy of the colliding particles and the steric effect. Very recently, Imura et al.[10] have studied the anisotropic interaction of halogen atom in C_2H_5X (X = Cl,F) with He* atom and found different trends in the interactions around the C−X (X = Cl,F) bond; the attractive interaction was dominant around the perpendicular directions to the C−Cl bond axis in good agreement with the results of Tokue et al.[7], whereas for the C−F bond, the attractive interaction was localized around the collinear axis. These differences between the Cl and F atoms can be ascribe to the presence of the different types of orbital interactions between the C and the Cl atoms and to the F atoms.

2D-PIES studies of F atom containing compounds with He*-(2^3S) atoms have been reported for fluoroethane,[10] monofluorobenzene,[11] and difluorobenzenes[12]. As suggested in these studies, if found only by the aid of the theoretical and/or semiempirical calculated ionization potentials (IPs), band assignments of the He I ultraviolet photoelectron spectrum (UPS) for the F atom containing compounds are quite difficult, and sometimes these methods make inappropriate band assignments. Similarly, for 1,3,5-$C_6H_3F_3$ and C_6F_6 molecules, the band assignments of He I UPS still remain doubtful.

In the present study, we reexamined the assignments for these molecules by using the characteristics of the 2D-PIES. Furthermore, to elucidate the relative reactivity of target MOs and also the absolute magnitude of interaction around the corresponding orbital region, we compared the present results with the other fluorobenzenes.[11,12] Such a comparison is of considerable chemical significance because it provides not only valuable knowledge of the substituent effect upon the reactivity of

10.1021/jp0124239 CCC: $20.00
Published on Web 11/10/2001

orbitals, but also important stereo-dynamical aspects of the Penning ionization.

II. Experimental Section

High purity samples of 1,3,5-$C_6H_3F_3$ and C_6F_6 were commercially purchased and purified by several freeze−pump−thawed cycles. The experimental apparatus for measurements of He*(2^3S) PIES and He I (584 Å, 21.22 eV) UPS has been reported previously.[13−16] Briefly, a metastable He*(2^1S,2^3S) beam was generated by a discharge, and the He*(2^1S) component was optically removed by a helium discharge lamp. He I UPS were measured by He I resonance photons produced by a discharge in pure helium gas. The kinetic energy of ejected electrons was measured by a hemispherical electrostatic deflection type analyzer. We estimate the energy resolution of the electron energy analyzer to be 70 meV from the full width at the half-maximum (fwhm) of the $Ar^+(^2P_{3/2})$ peak in the He I UPS. The observed PIES and UPS were calibrated by the transmission efficiency curve of the electron analyzer, which was alternatively determined by comparing our UPS data of several molecules with those by Gardner and Samson[17] and Kimura et al.[18] Calibration of the electron energy scale was made by reference to the lowest ionic state of N_2 mixed with the sample molecule in He I UPS (E_e = 5.639 eV)[19] and He* (2^3S) PIES (E_e = 4.292 eV).[20,21]

In the collision-energy-resolved experiments, 2D-PIES, the metastable atom beam was modulated by a pseudorandom chopper[22] rotating at about 400 Hz and introduced into the reaction cell located about 500 mm downstream from the chopper disk, keeping constant the sample pressure. The resolution of the electron analyzer was lowered to 250 meV in order to gain higher electron counting rates. Kinetic electron energies (E_e) were scanned by 35 meV steps. The 2D Penning ionization data as functions of both E_e and t were converted by Hadamard transformation in which time dependent signals were cross-correlated with the complementary slit sequence of the pseudorandom chopper, and then the velocity dependence of the electron signals was obtained. The velocity distribution of the metastable He* beam, $I_{He^*}(v_{He^*})$, was determined by measuring the intensity of secondary emitted electrons from the inserted stainless plate. The 2D Penning ionization cross section $\sigma(E_e,v_r)$ was obtained with normalization by the velocity distribution of the He* beam, where v_r is the relative velocity averaged over the velocity of the target molecule. Finally, $\sigma(E_e,v_r)$ is converted to $\sigma(E_e,E_c)$ as functions of E_e and E_c, where E_c is the collision energy of the colliding particles.

III. Calculations

We performed ab initio self-consistent field (SCF) calculations with 4-31G basis functions for 1,3,5-$C_6H_3F_3$ and C_6F_6 in order to obtain electron density contour maps of MOs. In electron density maps, thick solid curves indicate the repulsive molecular surface approximated by van der Waals radii[23] (r_C = 1.7 Å, r_H = 1.2 Å, r_F = 1.35 Å).

The ionization potentials were also calculated at the experimentally determined geometries[24,25] using the outer valence Green's function (OVGF) method[26,27] for 1,3,5-$C_6H_3F_3$ and C_6F_6 with 6-311G** and 6-311G basis sets, respectively.

Interaction potential energy surfaces between M and He*(2^3S) in various directions and distances were modeled by approximating the M-He(2^3S) surfaces with those of Li(2^2S)-M based on the well-known resemblance between He*(2^3S) and Li(2^2S);[28] similar shape for the velocity dependence of the total scattering cross section and for the location and depth of the attractive potential well for He*(2^3S) and Li(2^2S) with various

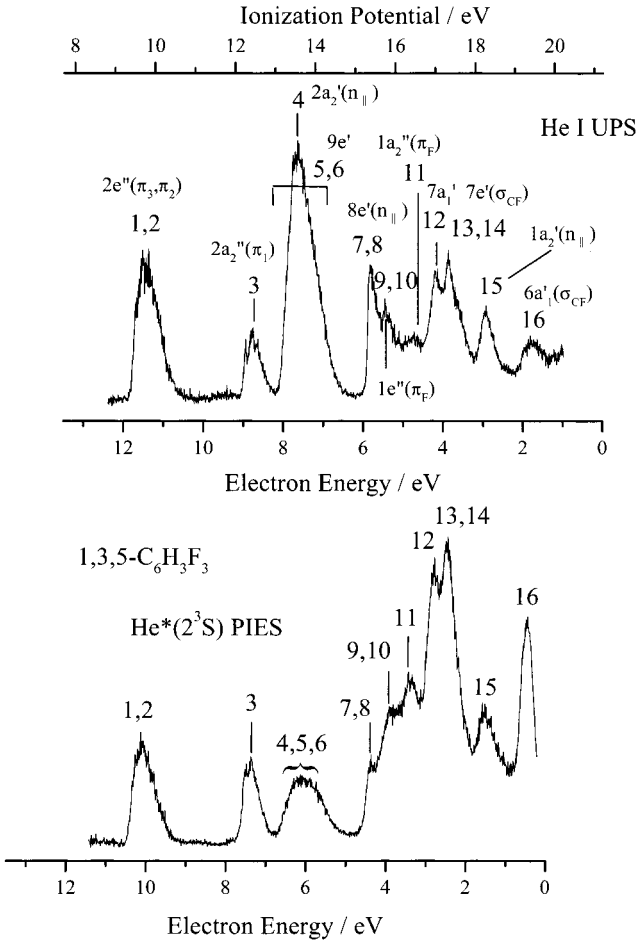

Figure 1. He I UPS and He*(2^3S) PIES of 1,3,5-$C_6H_3F_3$.

atomic targets.[29−32] Recently, a precise estimate of the similarity[33] has been made for atomic targets; the well depths for the Li + Y (Y = H, Li, Na, K, Hg) systems were found to be 1.1∼1.2 times larger than those for He*(2^3S) + Y. Although for molecular targets M, a direct comparison between the interactions of Li + M and He* (2^3S) + M has never been reported so far, the observed peak energy shifts between PIES and UPS, which were relevant to the interaction potentials between the reagents, were well-reproduced by the Li + M potentials calculations for numerous compounds.[34−38] Because of these findings and the difficulties associated with calculation for excited states, the Li was used in this study in place of He*(2^3S). Thus, the interaction potential M-Li(2^2S), $V^*(R)$ (where R is the distance between Li atom and either F atom or the center of the benzene ring), was calculated by moving the Li atom toward either F atom or the center of the benzene ring and keeping the molecular geometries fixed at the experimental values; this assumption meant that the geometry change during the approach of a metastable atom was negligible in the collisional ionization process. For calculating the interaction potential, the standard 6-31+G* basis set was used, and the electron correlation effect was partially taken into account by using second-order Møller−Plesset perturbation theory (MP2). All the calculations in this study were performed with the GAUSSIAN 98 quantum chemistry program.[39]

IV. Results

Figures 1 and 2 show the He I UPS and He*(2^3S) PIES of 1,3,5-$C_6H_3F_3$ and C_6F_6, respectively. The electron energy scale for PIES are shifted relative to those of UPS by the excitation

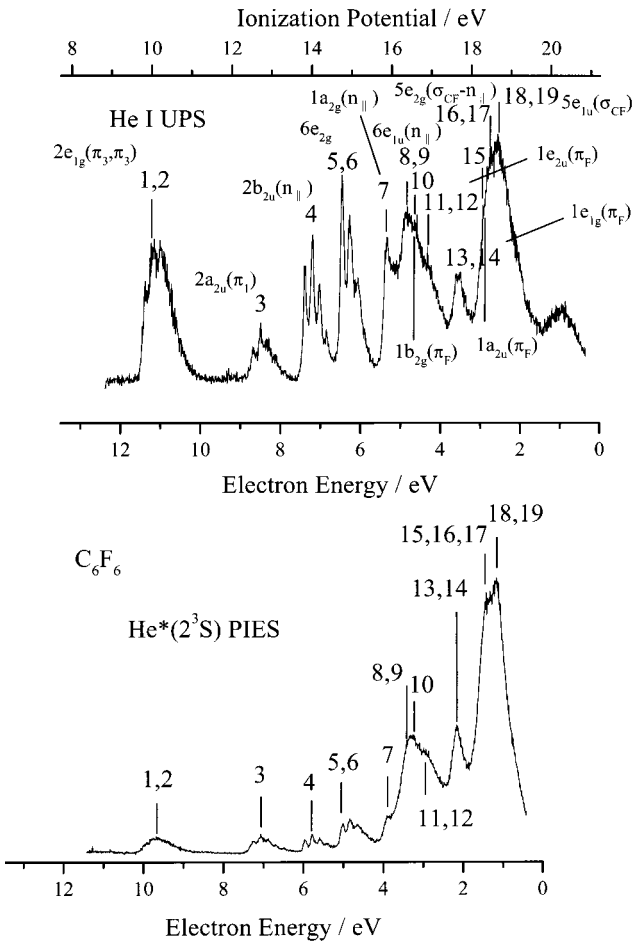

Figure 2. He I UPS and He*(2³S) PIES of C_6F_6.

energy difference between He I photons (21.22 eV) and He*-(2³S) (19.82 eV), namely, 1.40 eV. Band labels in UPS show orbital characters based on their symmetries and bonding characters.

Collision-energy-resolved PIES (CERPIES) obtained from the two-dimensional data for 1,3,5-$C_6H_3F_3$ and C_6F_6 are shown in Figures 3 and 4, respectively. The CERPIES are shown for low collision energy (ca. 100 meV) and for high collision energy (ca. 300 meV). The relative intensities of the two spectra are normalized in the figures using the data of the log σ versus log E_c plots.

Figures 5 and 6 show the log σ versus log E_c plots of CEDPICS in a collision energy range of 100−310 meV for 1,3,5-$C_6H_3F_3$ and C_6F_6 with the calculated electron density maps, respectively. The CEDPICS was obtained from the 2D-PIES $\sigma(E_e,E_c)$ within an appropriate range of E_e(typically electron energy resolution of analyzer, 250 meV) to avoid the effect of neighboring bands. The calculated electron density maps for σ orbitals are shown on the molecular plane, and those for π orbitals are shown on a plane at a height of 1.7 Å (van der Waals radii of C atom) from the molecular plane.

Tables 1 and 2 list experimentally determined ionization potentials (IPs) from the He I UPS, experimental peak energy shift (ΔE), slope parameters of CEDPICS (m), and the assignments of the bands. Valence IP values by the OVGF calculations and earlier reported semiempirical HAM/3 calculations[40] are also summarized in the tables. The peak energy shifts are obtained as the difference between the peak position (E_{PIES}; electron energy scale) and the "nominal" value (E_0 = difference between metastable excitation energy and sample IP): $\Delta E = E_{PIES} - E_0$. Slope parameters are obtained from the log σ versus log E_c plots in a collision energy range for 100−310 meV by a least-squares method.

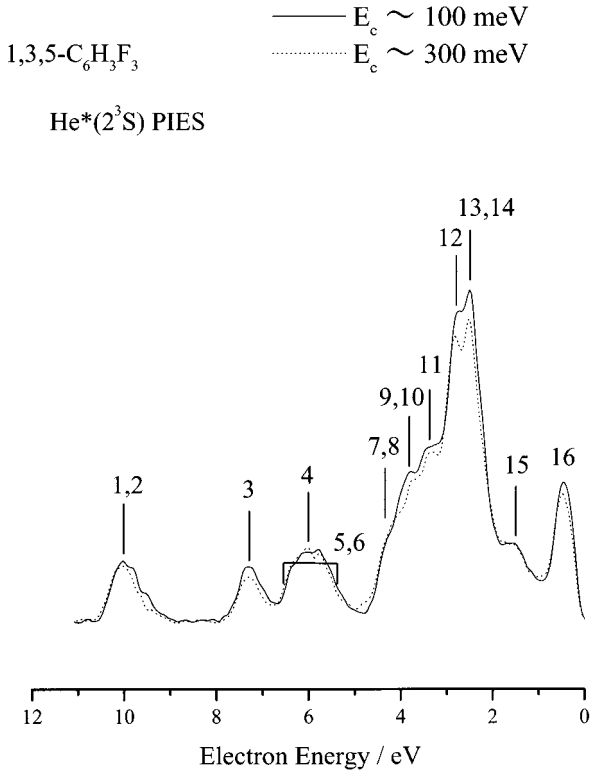

Figure 3. Collision-energy-resolved He*(2³S) PIES of 1,3,5-$C_6H_3F_3$. E_c denotes collision energy.

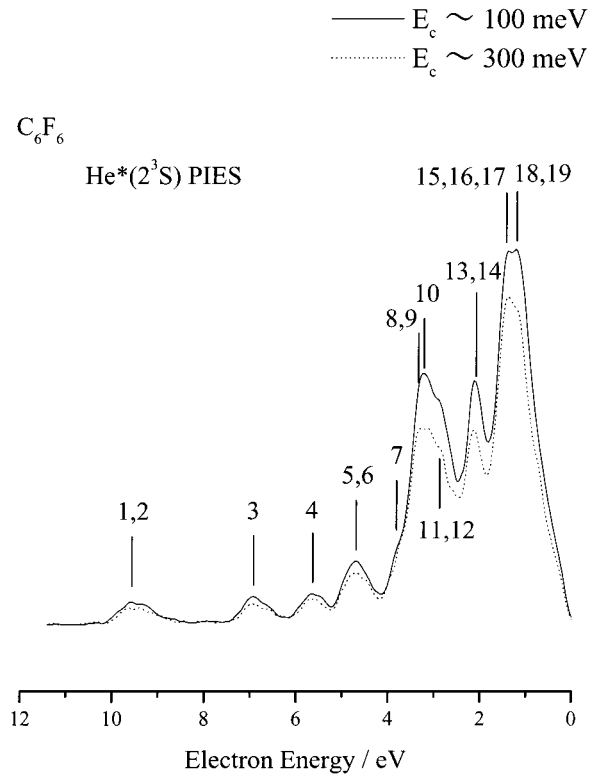

Figure 4. Collision-energy-resolved He*(2³S) PIES of C_6F_6. E_c denotes collision energy.

Calculated interaction potential energy curves between the Li(²S) atom and 1,3,5-$C_6H_3F_3$ and C_6F_6 by the MP2/6-31+G* level of theory are shown in Figures 7(a) and 7(b), respectively.

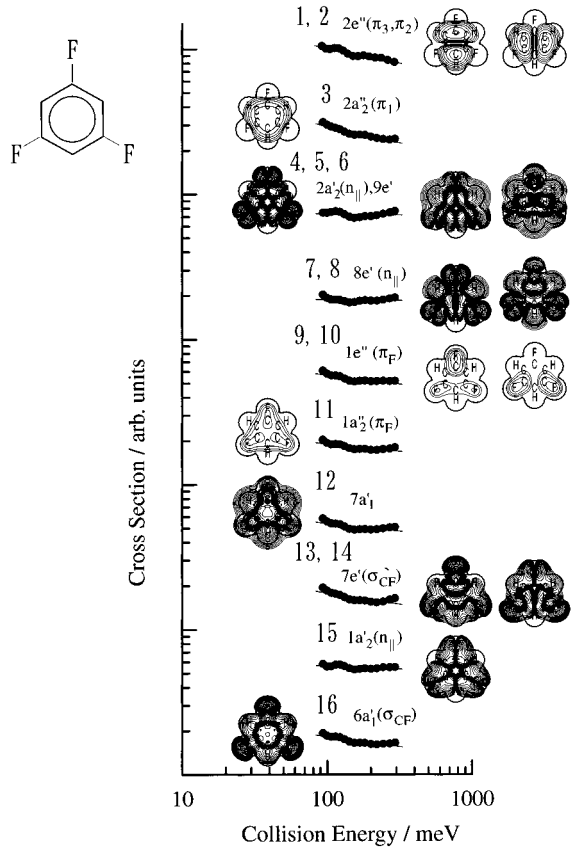

Figure 5. Collision energy dependence of partial ionization cross sections for 1,3,5-$C_6H_3F_3$ with He*(2^3S) atom. The contour plots show electron density maps for respective MOs.

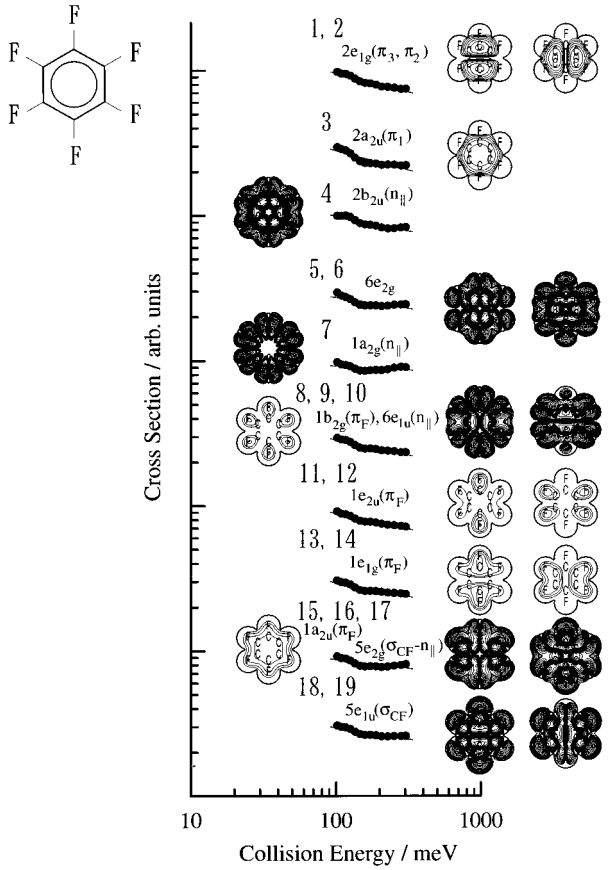

Figure 6. Collision energy dependence of partial ionization cross sections for C_6F_6 with He*(2^3S) atom. The contour plots show electron density maps for respective MOs.

The potential energy curves are shown as a function of the distance *R* between the Li and either F atom or the center of the benzene ring.

V. Discussion

Band Assignments and PIES Intensities. Photoelectron spectra of 1,3,5-$C_6H_3F_3$ and C_6F_6 have been extensively investigated.[40−47] The spectra of the fluorobenzenes are especially interesting because bands arising from F atom electrons are not expected to occur in the 9−13 eV region on account of the high IP of the F atom (17.42 eV). Thus, the $e_{1g}(\pi_{3,2})$ and $a_{2u}(\pi_1)$ orbitals of the benzene core which have IPs in this region are not interfered with nearby halogen bands and in fact can be identified unambiguously. On the other hand, one difficulty for assigning the spectra in the region 16−20 eV can be due to the fact that the atomic IP of fluorine is higher than that of the other halogen atoms and the lone pair ionization of the aliphatic fluoride occur in the region 16−20 eV. Therefore, some uncertainty has remained in the assignment in this region despite numerous studies, while only Bieri et al.[40] made comprehensive band assignments for these compounds. As previously demonstrated,[12] on the basis of the characteristics of the 2D-PIES which provides direct information on the spatial distribution of individual MOs and anisotropy of interactions, UPS bands can be assigned unambiguously.

Aoyama[48] studied PIES of these compounds and proposed their band assignments. However, more careful assignments are necessary by taking the result of the 2D-PIES experiment and the similarity to the monofluorobenzene[11] into account. PIES for 1,3,5-$C_6H_3F_3$ and C_6F_6 are shown in Figures 1 and 2 together with UPS, respectively. The branching ratios are clearly different when compared to those in UPS and reflect the difference in the ionization mechanism; strong bands in PIES originate from orbitals having large electron density exposed outside the molecular surface.

UPS and PIES of 1,3,5-$C_6H_3F_3$. Bands 1, 2, and 3 were assigned to ionization from $\pi_{3,2}$ and π_1 orbitals as proposed by previous studies[40,41] and also by the calculated IPs by the OVGF and HAM/3 method. In PIES, intensity of π_1 band is more enhanced than the one of $\pi_{3,2}$ band, when compared with the corresponding bands in UPS. This can be explained by the larger electron distribution of the π_1 orbital than that of the $\pi_{3,2}$ orbitals; electron distribution of the π_1 orbital is constructed by a combination of C 2p atomic orbitals in-phase, while the electron distributions of the π_3 and π_2 orbitals are composed of the out-of phase C 2p atomic orbitals. The latter distributions are separated by a nodal plane. A very strong peak appeared at IP $\approx$ 13.5 eV (band 4,5,6) in UPS turned out to be a weak band in PIES. In the case of monofluorobenzene,[11] the corresponding peak was observed at IP = 13.90 eV in UPS and assigned as $n_{||}$ (nonbonding orbital mostly due to fluorine 2p orbital directed perpendicular to the C−F bond axis distributed in-plane to the benzene ring) orbital. Moreover, sharp peaks appeared at IP $\approx$ 15.4 eV (bands 7,8) and at IP $\approx$ 18.3 eV (band 15) in UPS are typical observation due to ionization from nonbonding MOs, and they were observed as weak peaks in PIES. Then, we related them (bands 7, 8, and 15) to the ionization from $n_{||}$ orbitals. Weak PIES intensities for these bands can be explained from a steric shielding effect of the benzene ring. Namely, the benzene ring spatially prevents reactive trajectories of He* toward F atoms resulted in smaller ionization probability. Such a shielding effect of bulky groups has been previously observed in several other compounds.[49−51]

TABLE 1: Band Assignment, Ionization Potentials (IP/eV), Peak Energy Shifts (Δ*E*/meV), and Slope Parameters (*m*) for 1,3,5-$C_6H_3F_3$.

band	IP_{obsd}/eV	IP_{OVGF}/eV (pole strength)	HAM/3[a] IP/eV	orbital character	Δ*E*/meV	*m*
1,2	9.69	9.70(0.91)	10.08	2e"(π_3, π_2)	-30 ± 60	−0.21
3	12.46	12.64(0.86)	11.98	$2a_2$"(π_1)	0 ± 40	−0.23
4	13.57	13.99(0.90)	13.35	$2a_2'(n_{\|\|})$	−	−0.02
5,6	(13.2−14.3)	13.86(0.91)	13.73	9e′	−	
7,8	15.40	15.94(0.90)	15.25	8e′($n_{\|\|}$)	-30 ± 50	−0.02
9,10	15.76	16.94(0.89)	16.03	1e"(π_F)	-100 ± 50	−0.12
11	16.49	17.20(0.86)	16.49	$1a_2$" (π_F)	$(+20 \pm 80)$	−0.10
12	17.00	17.47(0.89)	16.82	$7a_1'$	0 ± 40	−0.11
13,14	17.34	17.65(0.88)	17.10	7e′(σ_{CF})	0 ± 40	−0.16
15	18.29	18.63(0.88)	17.30	$1a_2'$ ($n_{\|\|}$)	-10 ± 60	−0.04
16	19.41	19.81(0.88)	18.88	$6a_1'$ (σ_{CF})	$+30 \pm 80$	−0.15

[a] Reference 40.

TABLE 2: Band Assignment, Ionization Potentials (IP/eV), Peak Energy Shifts (Δ*E*/meV), and Slope Parameters (*m*) for C_6F_6.

band	IP_{obsd}/eV	IP_{OVGF}/eV (pole strength)	HAM/3[a] IP/eV	orbital character	Δ*E*/meV	*m*
1,2	10.00	10.00(0.91)	10.68	$2e_{1g}(\pi_3, \pi_2)$	-100 ± 70	−0.26
3	12.73	12.93(0.87)	12.30	$2a_{2u}(\pi_1)$	-20 ± 40	−0.26
4	14.03	14.27(0.91)	13.72	$2b_{2u}(n_{\|\|})$	-10 ± 40	−0.20
5,6	14.76	15.21(0.90)	14.74	$6e_{2g}$	-50 ± 40	−0.15
7	15.88	16.53(0.90)	15.61	$1a_{2g}(n_{\|\|})$	-30 ± 60	−0.05
8,9	16.39	16.82(0.90)	15.81	$6e_{1u}(n_{\|\|})$	(-10 ± 90)	−0.19
10	16.64	17.19(0.90)	15.88	$1b_{2g}(\pi_F)$	$(+20 \pm 90)$	
11,12	16.90	17.42(0.90)	16.16	$1e_{2u}(\pi_F)$	(-50 ± 90)	−0.20
13,14	17.63	18.14(0.89)	17.23	$1e_{1g}(\pi_F)$	-20 ± 70	0.18
15	(18.28)	18.77(0.82)	18.21	$1a_{2u}(\pi_F)$	$(+80 \pm 120)$	−0.12
16,17	18.46	18.93(0.90)	18.18	$5e_{2g}(\sigma_{CF}\text{-}n_{\|\|})$	$+40 \pm 80$	
18,19	18.66	19.11(0.89)	18.48	$5e_{1u}(\sigma_{CF})$	$+20 \pm 70$	−0.18
	(20.2)	20.36(0.89)	20.10	$4b_{1u}(\sigma_{CF})$		
		20.74(0.88)	19.18	$5a_{1g}$		
		21.12(0.88)	19.39	$1b_{2u}$		

[a] Reference 40.

A weak and broad band appeared at IP ≈ 13.5 eV and was assigned to the overlapping $n_{||}$ and σ_{CH} bands because of the following reasons: (1) Although, in general, $n_{||}$ band appeared as sharp peak in UPS, the rise of this band at high E_e region shows rather mild increase compared with the other $n_{||}$ bands (bands 7,8). This observation suggests that the $n_{||}$ band (band 4) is overlapped with a broad band. (2) Bands 5,6 are degenerate orbitals having σ_{CH} characters; therefore, it is expected that the Jahn−Teller splitting becomes important for these orbitals. As shown in Figure 3, shoulders arising from bands 4 and 5,6 can be seen near the peak appeared at $E_e \approx 6.05$ eV ($n_{||}$ band), which may be due to bands splitting by the Jahn−Teller effect. In addition, being similar to the case of the monofluorobenzene the $n_{||}$ and σ_{CH} orbitals shows weak PIES intensities.[11,52] (3) OVGF calculation provided equivalent IPs of these bands, 13.99 eV for $2a_2'(n_{||})$ and 13.86 eV for 9e′orbital. By taking these features (1)−(3) into account, it is reasonable to assign the band appeared at IP ≈ 13.5 eV to be overlapping bands 4 and 5,6.

π_F (out-of-plane fluorine 2p orbital conjugated with some of carbon 2p orbitals in benzene) band in PIES of the monofluorobenzene showed relatively strong PIES intensity around $E_e \approx 4$ eV. Being similar to the case of monofluorobenzene and difluorobenzenes,[12] relatively strong PIES intensity of 1,3,5-$C_6H_3F_3$ around $E_e \approx 4-3$ eV were observed and assigned to two π_F bands (bands 9,10 and 11) based both on the OVGF calculations and on the latter discussions. It is noted that intensity of bands 9,10(1e"(π_F)) is larger than that of band 11 ($1a_2$"(π_F)) in UPS. This is because bands 9,10 are ionization from degenerate orbitals, whereas band 11 is ionization from a single orbital. On the other hand, in PIES intensity of band 11 is larger than that of bands 9,10. This can be explained by the larger electron density of $1a_2$"(π_F) orbital compared with the 1e"(π_F) orbitals. It has to be noted that the electron densities of 1e"(π_F) orbitals are segmented by a nodal plane, whereas that of $1a_2$"-(π_F) orbital is not. These findings further support the assignments of bands 9,10 and 11. In PIES, three very strong peaks were observed around $E_e \approx 2.5$ and ∼0.5 eV regions. In accord with these findings, very strong peaks were observed near the corresponding region ($E_e \approx 3.0-1.0$ eV) for the difluorobenzenes. These very strong peaks were assigned to be ionization from MOs having a σ_{CF} orbital character. (σ_{CF} is bonding orbital mostly due to the fluorine 2p orbital with the collinear direction to C−F bond axis.) We related two of three strong bands to σ_{CF} orbitals such as band 13, 14, and 16 based on the similarity of the CEDPICS for these bands as discussed later. These strong PIES intensities are explained by large electron distribution exposed outside the repulsive surface. The remaining very strong peak near $E_e \approx 4.3$ eV labeled as band 12, therefore, can be related to the $7a_1$ orbital. The observed strong intensity of this band can be related to the overlapping with the strongest band (bands 13,14). It is also noted that the electron distribution outside the molecular surface of $7a_1'$ orbital is not separated by a nodal plane. Then, ionization from this MO is expected to be large, similarly to the case of π_1 orbital mentioned above.

Proposed band assignments in UPS agree with the ones reported by Bieri et al.[40] based on the semiempirical HAM/3 calculation, while Bieri et al. did not discuss the band feature of bands 4 and 5,6. Although the OVGF calculation reproduces the order of a band sequence, differences of observed and calculated IPs for bands 9, 10, and 11 are more than 0.7 eV. Moreover, for low (bands 1, 2, and 3) and high (bands 15 and 16) IPs, better agreement between the calculated IPs and observed ones was found for the OVGF method than for the HAM/3 calculation, while for bands 5−14 opposite result was found. These results indicate the difficulty of band assignments in UPS by calculations alone.

UPS and PIES of C_6F_6. Bands 1,2, 3, 4, and 5,6 were assigned as ionization from $2e_{1g}(\pi_{3,2})$, $2a_{2u}(\pi_1)$, $2b_{2u}(n_{||})$, and $6e_{2g}$ orbitals in accord with the assignments of Bieri et al.[40] and also with the calculated IPs by the OVGF and HAM/3 methods. The calculated IPs for these orbitals by the OVGF method reproduced the observed IPs within 0.5 eV. Vibrational population patterns of bands 5,6 are clearly different between UPS and PIES; vibrational excitation was found to be much pronounced for PIES. From the analysis of vibrational frequency (1510 cm^{-1}) of this band,[43] these vibrations was assigned to C−F stretching vibration. Thus, the vibrational excitation in PIES implies that the C−F bond is extended by the collinear approach of the He* atom along the C−F bond. This is consistent with the electron distribution of $6e_{2g}$ orbital. In PIES, π_1 band is enhanced with respect to the other bands (bands 1, 2, 4, and 5,6). This observation can be ascribed to the larger electron density around the phenyl ring region for the π_1 orbital. A sharp peak appeared at IP $\approx$ 15.8 eV in UPS (band 7) can be related to the ionization from nonbonding type orbital. In PIES, this was observed as a weak band being similar to band 4 ($2b_{2u}$-($n_{||}$) orbital). Thus, it can be related to the $n_{||}$ type orbital because the electron distribution outside the repulsive surface is effectively shielded by both the F atoms and the phenyl ring.

The remaining bands in the lower E_e region (< 3.8 eV) in PIES show very strong intensities, especially, at $E_e \approx 1.2$ eV region. The strongest peaks labeled as 18,19 in PIES can be assigned to ionization from σ_{CF} orbitals because the electron density distribution of the orbitals extends over the larger region as in the case of 1,3,5-$C_6H_3F_3$. For C_6F_6, there are six C−F bonds, and thus electron density around the F atoms in σ_{CF} type orbital is larger than that of 1,3,5-$C_6H_3F_3$. As a consequence, a considerably strong band was observed. The shoulders (band 15 and bands 16,17) of the bands 18,19 can be related to $1a_{2u}$-(π_F) and $5e_{2g}$(σ_{CF}-$n_{||}$) orbitals, since σ_{CF} type orbitals give strong PIES intensities as mentioned above. Moreover, electron density of $5e_{2g}$(σ_{CF}-$n_{||}$) orbitals along the C−F bond is smaller than that of $5e_{1u}$(σ_{CF}) orbitals. In other words, $5e_{2g}$(σ_{CF}-$n_{||}$) orbitals have $n_{||}$ characters, while $5e_{1u}$(σ_{CF}) orbital does not. Thus, it is expected for $5e_{2g}$(σ_{CF}-$n_{||}$) orbitals to give smaller intensity than for $5e_{1u}$(σ_{CF}) orbitals. Because electron density of $1a_{2u}$(π_F) orbital is distributed over the large region, $1a_{2u}$(π_F) orbital also gives relatively strong PIES intensity. Strong bands labeled as 11,12 and 13,14 were assigned to $1e_{2u}$(π_F) and $1e_{1g}$(π_F) orbitals, respectively. Stronger PIES intensity of bands 13,14 than that of bands 11,12 can be explained by the fact that electron densities of $1e_{1g}$(π_F) orbitals are larger than those of $1e_{2u}$(π_F) orbitals. Electron densities of $1e_{2u}$(π_F) orbitals are separated by nodal planes, whereas those of $1e_{1g}$(π_F) orbitals are not. In UPS, intensity of bands 8,9 is larger than that of band 10. It may indicate that the bands 8,9 are ionization from degenerate orbitals. Although bands origins of 8,9 and 10 are not clearly observed in PIES as shown in Figure 2, CERPIES partially resolved the band structures as can be seen in Figure 4. We assigned the higher edge and major contribution of this band in electron energy scale to be due to ionization from $6e_{1u}$($n_{||}$) and $1b_{2g}$(π_F) orbitals, respectively, because the π_F band gives larger intensity compared to the $n_{||}$ band.

These assignments of the band in He I UPS for C_6F_6 are in agreement with those of Bieri et al.[40] except for assignments of bands 15−17. In addition, they did not resolved several band origins around IP = 16.2∼17.0 and 18.1∼19.0 eV regions in UPS.

Collision Energy Dependence of the Partial Ionization Cross Sections (CEDPICS). *(i) 1,3,5-$C_6H_3F_3$.* Positive or negative slope of CEDPICS reflects the characteristics of interaction between the colliding particles. In the case of attractive interaction, a slower He* metastable atom can approach the reactive region effectively by attractive force, and then, ionization cross section is enhanced for lower collision energies. Relatively strong ($m < -0.10$) negative collision energy dependence of partial ionization cross section was observed for $\pi_{3,2,1}$, π_F, and σ_{CF} bands. It implies that the ionization around these orbitals regions were governed by the attractive interaction with the He* atom. Calculated interaction potentials shown in Figure 7(a) also indicate the attractive interactions for the corresponding regions. Namely, attractive interactions were found for the collinear direction to the C−F bond axis at short inter-nucleus (F−Li atom) distance (∼2 Å, 18 meV) and for the π orbital regions at long distance (∼4 Å, 46 meV) between a Li atom and the center of mass of the molecule. The latter attractive potential wells extend over the wider region. Therefore, observation of the strongest negative CEDPICS of $\pi_{3,2}$ and π_1 bands can be related to the wider and deeper attractive potential for the phenyl ring region.

Repulsive interactions result in positive m values of the CEDPICS reflecting the fact that a faster He* atom can approach inner reactive regions effectively against the repulsive potential wall. Smaller absolute m values of CEDPICS were found for the bands 7,8, and 15, which were assigned to $n_{||}$ type orbitals, and it indicates that ionization events from these MOs are governed by a slightly repulsive or attractive interaction around the $n_{||}$ orbital region with the He* atom. This is consistent with the relatively weak PIES intensities of these bands, whereas the same argument cannot be easily applied to band 4 due to the overlapping with a broad neighboring band. Moreover, calculated potential curve (■) in Figure 7(a) shows a repulsive interaction for this orbital region, which also support the validity of the above argument.

Because the m values of the CEDPICS depend on the contributions of the attractive and the repulsive interactions around the molecule, the MOs having equivalent orbital characters show a quite similar value m of CEDPICS each other. An interesting feature of CEDPICS for bands 7,8 and 12 was found; ionization cross sections of these bands decrease with increasing collision energy for lower collision energy region and increase for higher collision energy region. The decline for the lower collision energy region can be ascribed to the attractive interaction around the collinear direction along the C−F bond because the corresponding orbitals have electron density outside the repulsive surface around the collinear direction to the C−F bond. The positive slope for the higher collision energy can be related to the repulsive interaction around either C−H bonds or the $n_{||}$ orbital region. The ordering of slope parameter of CEDPICS can be summarized as $m(\pi_{3,2,1}) < m(\sigma_{CF}) < m(\pi_F) < m(n_{||})$. These results indicate that the measurement of CEDPICS is a powerful tool to make reliable band assignments in UPS.

(ii) C_6F_6. Slope parameters of CEDPICS for all bands show negative values. Generally, the tendency of the anisotropic interaction around molecule was identical to the case of 1,3,5-$C_6H_3F_3$, whereas the absolute m value of CEDPICS for each band is slightly larger than the corresponding one for1,3,5-$C_6H_3F_3$. This finding suggests that interactions of each MO region upon the electrophilic attack of the He* atoms in C_6F_6 are qualitatively similar to the interactions in 1,3,5-$C_6H_3F_3$ molecules, although the magnitude may be slightly different each other. Qualitatively similar interaction potential around the molecule is also supported by the theoretical calculation as recognized their similarity between the calculated interaction

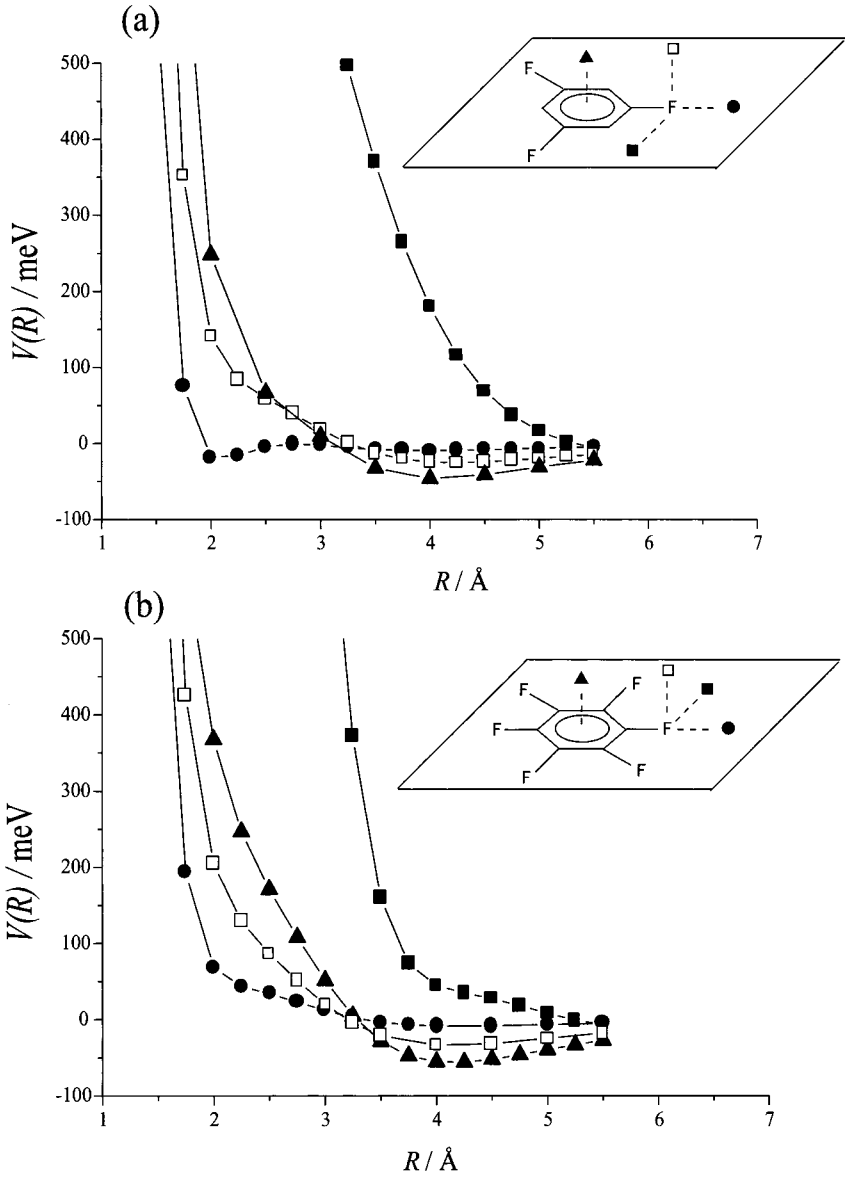

Figure 7. Interaction potential curves $V(R)$ obtained by MP2 calculations for the target molecules and Li atom as a function of distance R; out-of-plane access to the center of the benzene ring (▲); in-plane collinear access to the C−F bond (●); in-plain perpendicular access to the C−F bond (■); out-of-plane perpendicular access to the C−F bond (□). Note that R is defined from the center of the benzene ring for (▲) direction, whereas for the others (●), (■), (□) R is defined from the F atom. (a) for 1,3,5-$C_6H_3F_3$ (b) for C_6F_6.

potentials of 1,3,5-$C_6H_3F_3$ and C_6F_6 with Li atom as shown in Figures 7(a) and 7(b), whereas attractive interaction was not found for the collinear direction (●) in Li−C_6F_6 system contrary to the case of Li-1,3,5-$C_6H_3F_3$ system. However, experimental results indicate that the attractive effect for the corresponding region for C_6F_6 is slightly larger or comparable compared to the 1,3,5-$C_6H_3F_3$ because the absolute value ($m(\sigma_{CF}) = -0.18$) of the σ_{CF} bands corresponding to the collinear direction (●) region for C_6F_6 is slightly larger or comparable to the one ($m(\sigma_{CF}) = -0.15$) for 1,3,5-$C_6H_3F_3$. We have also performed B3LYP/6-31+G* calculation of the collinear direction for the Li−C_6F_6 system and actually found that the attractive well depth of 15.5 meV at 2.0 Å inter-nucleus distance between Li and F atom. The discrepancy between the observation and the MP2/6-31+G* calculation may be reduced by utilizing larger basis set for the Li−C_6F_6 system. Details of attractive interactions around the π_1, π_F, $n_{||}$, and σ_{CF} orbitals regions will be discussed later.

Comparison with the other Fluorobenzenes. *(i) Reactivity of the Orbitals.* The substituent effect on the reactivity of orbitals and anisotropic interaction around the molecule has been studied through the 2D-PIES measurements of monofluorobenzene[12] and difluorobenzenes[11]. For the purpose of obtaining better insight into the role of the substituent effect, we will discuss the relative reactivity and anisotropic interaction around the $\pi_{3,2,1}$, π_F, $n_{||}$, and σ_{CF} orbitals region of the fluorobenzenes on the basis of the relative PIES intensities and slope parameters of the $\pi_{3,2,1}$, π_F, $n_{||}$, and σ_{CF} bands in CEDPICS.

The relative band intensities of π_1, π_F, $n_{||}$, and σ_{CF} bands in monofluorobenzene, difluorobenzenes, 1,3,5-trifluorobenzne, and hexafluorobenzene were obtained with respect to the intensity of the average of the π_3 and π_2 bands as a reference. Because the π_3 and π_2 bands are partially or completely overlapped with each other for these compounds, the average electron density distribution of the π_3 and π_2 orbitals among these compounds seems to be equivalent. Band intensity means the integrated intensity of the band. $I(n_{||})$ was evaluated from the $n_{||}$ band having lowest IP for mono-, di-, and hexa-fluorobenzenes and from the bands 7,8 for 1,3,5-$C_6H_3F_3$ because these bands are fairly well resolved compared to the other $n_{||}$

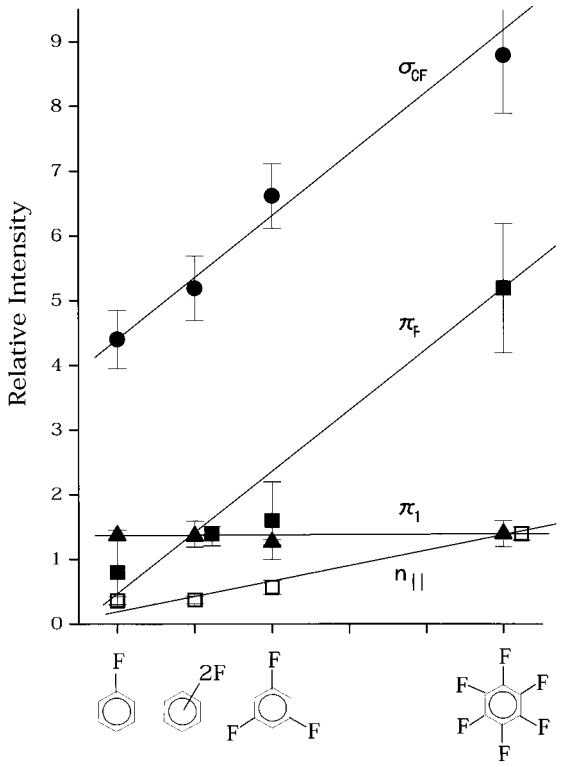

Figure 8. Relative PIES intensities of the π_1(▲), π_F(■), $n_{||}$(□), and σ_{CF}(●) bands with respect to the average intensity of the π_3 and π_2 band for C_6H_5F, $C_6H_4F_2$, 1,3,5-$C_6H_3F_3$, and C_6F_6. Estimated relationships were indicated by solid lines.

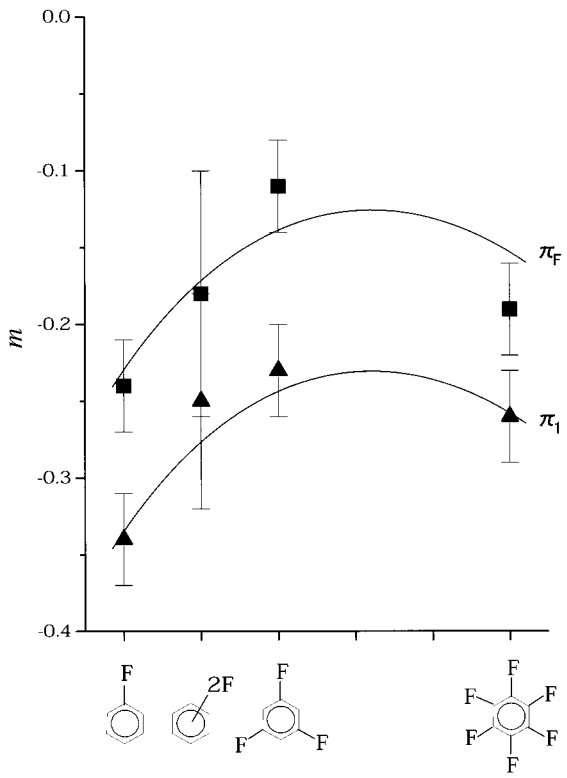

Figure 9. Obtained slope parameters of the π_1(▲) and π_F(■) bands for C_6H_5F, $C_6H_4F_2$, 1,3,5-$C_6H_3F_3$, and C_6F_6. The smaller value implies the larger attractive effect. The solid lines were estimated correlation among the compounds investigated.

bands among the compounds. Although there are bands characterized to either σ_{CF} or π_F bands, these bands are partially or seriously overlapped with neighboring bands having mainly identical orbital characters. Thus, $I(\sigma_{CF})$ and $I(\pi_F)$ were estimated as the average intensity of σ_{CF} and π_F bands, respectively. For partially overlapped bands, proper de-convolution was performed when necessary. Errors are mainly originated through this procedure. Large error for the $I(\pi_F)$ in the monofluorobenzene can be attributed to the uncertainly owing to the serious overlapping with this band and neighboring bands. For the difluorobenzenes, relative reactivity of orbitals among *o*-, *m*-, and *p*-$C_6H_4F_2$ molecules are averaged out. Relative intensities, $I(\pi_1)/I(\pi_{3,2})$, $I(\pi_F)/I(\pi_{3,2})$, $I(n_{||})/I(\pi_{3,2})$, and $I(\sigma_{CF})/I(\pi_{3,2})$, for the several compounds were shown in Figure 8. It is apparent that the reactivity of the orbitals becomes large with increasing the number of F atom substitutions except for the π_1 orbital. Nonincreasing behavior for the π_1 orbital was found within experimental errors, which can be explained by the small F atomic orbital component in the electron density of the π_1 orbital. This finding also supports the validity of the criterion choosing the average intensity of the π_3 and π_2 bands as a reference. As mentioned previously, reactivity of π_1 orbital is about 1.2−1.4 times larger than the average of π_3 and π_2 orbitals. Increasing behavior for the π_F and σ_{CF} orbital by the F atom substitution is quite large, and it is almost linearly increasing with the F atom substitution. This can be related to the increasing of the electron density especially around the F atoms with increasing the substitution. On the other hand, a very small increase was found for the reactivity of $n_{||}$ orbital. This finding again indicates the importance of the shielding effect for the ionization from this orbital.

(ii) Anisotropic Interaction around the Molecules. The slope parameters *m* of CEDPICS will be used for investigating the magnitude of interaction around the molecule because the *m* value is closely related to the shape of the potential energy surface around the ionization point and also to the interaction potential around the molecule. The *m* values for π_1 and π_F bands and σ_{CF} and $n_{||}$ bands are plotted in Figures 9 and 10, respectively. Here, we used the slopes obtained by the experiments without any normalization, and therefore, a direct comparison is possible. The $m(n_{||})$ was taken from the $n_{||}$ band having lowest IP for mono-, di-, and hexa-fluorobenzenes and from the bands 7,8 for 1,3,5-$C_6H_3F_3$ because of smaller overlapping with neighboring bands compared to the other $n_{||}$ bands. Some of π_F bands is overlapped mainly with the other π_F bands, and then the $m(\pi_F)$ was evaluated as the average of the π_F bands. The value of the σ_{CF} band is employed as that of the σ_{CF} band having highest IP in UPS because this band is fairly well resolved compared to the other σ_{CF} band, and electron distribution of the corresponding MO is similar to each other among the compounds. For the difluorobenzenes, the values among *o*-, *m*-, and *p*-$C_6H_4F_2$ molecules are averaged out.

The *m* values for π_1 and π_F bands are plotted in Figure 9. From the figure, several important propensities can be obtained. (1) The observed trends appear quite similar to each other, whereas (2) the absolute values of π_1 bands are always larger than the ones of π_F bands. (3) Absolute values of slope parameters for the π_1 and π_F bands decrease with increasing the numbers of F atoms from C_6H_5F to 1,3,5-$C_6H_3F_3$, and (4) slightly increase from 1,3,5-$C_6H_3F_3$ to C_6F_6. This finding (1) is closely related to the similarity of the electron distribution of these orbitals, whereas electron density around the F atoms and phenyl ring of the π_F orbital is larger and smaller compared to the electron density of the π_1 orbital, respectively. The finding (2) implies that the attractive effect is larger for the π_1 orbital region than for the π_F orbital region. The smaller attractive effect for the π_F orbital region than for the π_1 orbital region can be related to the larger electron density around F atoms and smaller

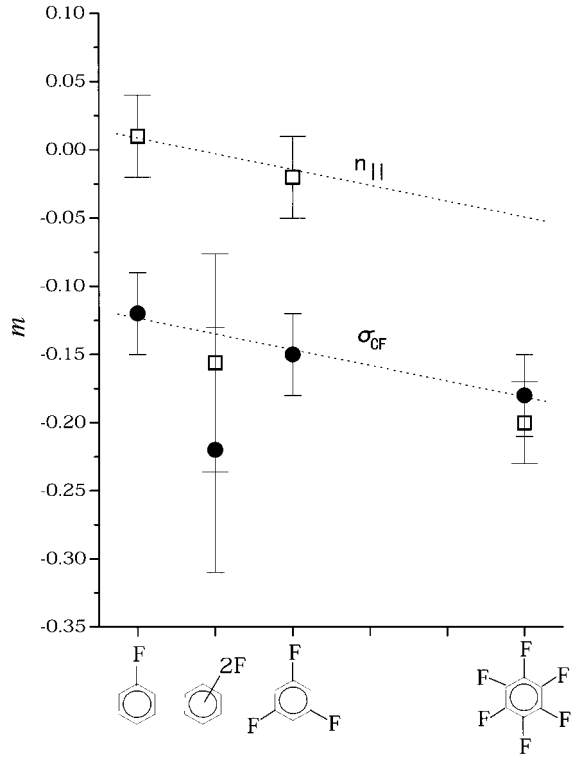

Figure 10. Obtained slope parameters of the $n_{||}$(□), and σ_{CF}(●) bands for C_6H_5F, $C_6H_4F_2$, 1,3,5-$C_6H_3F_3$, and C_6F_6. The smaller value implies the larger attractive effect. Definitions of the dashed curves see in the text.

electron density around the phenyl ring region as mentioned above. Namely, attractive effect around F atom lone pair region perpendicular to the phenyl ring is smaller than that around the phenyl ring region. This is consistent with the calculated interaction potentials for these regions as can be seen in Figure 7. The finding (3) implies the magnitude of attractive interaction decreasing with the increment of the substitution. This can be explained by the decreasing effect for electron density of the π_1 orbital with increasing the F atom substitution. Because the F atom is very strong electron-withdrawing substitute and then electron density of the π_1 orbital decreases with increasing the substitution. As a result, attractive interaction becomes smaller with increasing the F atom substitution. It is not apparent but decreasing effect on electron density of the π_1 orbital for these compounds can be seen in the density maps. It is also noted that reactivity of this orbital is actually slightly decreasing from C_6H_5F ($I(\pi_1)/I(\pi_{3,2}) = 1.37 \pm 0.08$) to 1,3,5-$C_6H_3F_3$ ($I(\pi_1)/I(\pi_{3,2}) = 1.26 \pm 0.10$) although the difference is smaller than experimental error. Finally, the finding (4) can be ascribed to the larger attractive effect around F atom lone pair region perpendicular to the phenyl ring for C_6F_6 than the effect for 1,3,5-$C_6H_3F_3$. It is noted that the corresponding region shows basically weak attractive interaction as indicated by the calculated interaction potentials in Figures 7(a) and 7(b); well depths are 46 and 55 meV for 1,3,5-$C_6H_3F_3$ and C_6F_6, respectively. The close proximity of F atoms in C_6F_6 can make wider attractive region compared to the 1,3,5-$C_6H_3F_3$. Therefore, larger attractive effect was expected for the F atom lone pair region perpendicular to the symmetry plane in C_6F_6 than the effect for the corresponding region in 1,3,5-$C_6H_3F_3$. Increment of the attractive effect for the π_1 band on going from 1,3,5-$C_6H_3F_3$ to C_6F_6 is also an indication of the larger attractive nature around the F atom lone pair region because the π_1 orbital has negligible F atomic components outside the repulsive surface. The attractive interaction of π_F bands is a combination effect of the attractive interactions around the phenyl ring and the F lone pair regions. Thus, this finding also indicates that the attractive effect around F atom lone pair region perpendicular to the phenyl ring is smaller than that around the phenyl ring region.

Figure 10 shows the values *m* of slope parameters for the $n_{||}$ and σ_{CF} bands. As it has been reported,[12] the attractive interactions for $n_{||}$ and σ_{CF} region in *o*-$C_6H_4F_2$ exhibit quite large "*neighboring group effect*", and this can be ascribed to the wider attractive potential well for these orbitals region. Thus, large absolute values, $m(\sigma_{CF}) = -0.35$ and $m(n_{||}) = -0.22$, of the *o*-$C_6H_4F_2$ elevated the average values of the difluorobenzenes for these bands. It is important to mention that the value $m(n_{||}) = -0.20$ of band 4 in C_6F_6 is very close to that of the *o*-$C_6H_4F_2$. This can also be ascribed to the *neighboring group effect*, namely closely spaced F atoms generate larger attractive region in C_6F_6 as the case of the *o*-$C_6H_4F_2$. It is also noted that the value of the other $n_{||}$ band (band 7) in C_6F_6 is quite small $m(n_{||}) = -0.05$ and very close to the one for C_6H_5F ($m(n_{||}) = +0.01$) and 1,3,5-$C_6H_3F_3$ ($m(n_{||}) = -0.02$). This is because the $1a_{2g}$-($n_{||}$) orbital (band 7) in C_6F_6 has no electron density at the midway between the close proximity of two F atoms, where the *neighboring group effect* plays a dominant role. Lack of observation similar to the *neighboring group effect* for the σ_{CF} band in C_6F_6 can also be related to the smaller electron density around the region, where the *neighboring effect* is dominant, compared to the case of *o*-$C_6H_4F_2$.

Assuming that the values for the difluorobenzene and the value of band 4 for C_6F_6 are regarded as exceptions, absolute values of the $n_{||}$ and σ_{CF} bands slightly increase by the F atom substitution as indicated by the dashed lines in the figure. It is also noted that the value (−0.14) of σ_{CF} band for *m*-$C_6H_4F_2$ is close to the estimated dashed curve denoted in the figure.

These results indicate that trajectories of the He* atom, which are responsible for the reaction, should be affected by interaction only in the narrow region near the reaction point. In the cases of the σ_{CF} and $n_{||}$ orbitals, the trajectory of the He* atom is only affected by interaction around a F atom located nearest to the reaction point. This is also closely related to the lack of observations of the *neighboring group effect* for the $1a_{2g}(n_{||})$ and σ_{CF} bands in C_6F_6. It is also noted that the order of the calculated well depth for the collinear direction (σ_{CF} orbital region) along the C−F bond for the fluorobenzenes by the MP2/6-31+G* level becomes mono-(∼100 meV) > di-(∼65 meV) > 1,3,5-tri (∼18 meV) > hexa- (∼−60 meV). This is closely correlated to the lowest IP of σ_{CF} orbital; mono-(16.64 eV) > *m*-di-(17.00 eV) > 1,3,5-tri (17.34 eV) > hexa- (18.46 eV). This correlation can be explained by the fact that an interaction of F atom with the 2s orbital of the He* atom becomes more effective to give attractive interaction with decreasing the IP of σ_{CF} orbital. Similar correlation was found for the π orbital.[36] Thus, small increment of absolute values $m(\sigma_{CF})$ of slope parameters for σ_{CF} bands on going from mono- to hexa-fluorobenzenes indicates that the attractive effect becomes slightly larger with increasing the number of F atoms owing to the increment of the attractive sites.

VI. Conclusion

In this study, we have measured the 2D-PIES of 1,3,5-$C_6H_3F_3$ and C_6F_6 with metastable He*(2^3S) atom. The results indicate highly anisotropic interactions around the molecules; Attractive interactions were found around the phenyl ring and σ_{CF} orbitals regions, whereas the ionization from the $n_{||}$ orbital region was

governed by a slightly repulsive or attractive interaction. By using the characteristics of 2D-PIES, we have proposed band assignments of He I UPS for the molecules. Furthermore, we discussed the substituent effect on the reactivity of π_1, π_F, $n_{||}$, and σ_{CF} orbitals and also on the magnitude of the interaction around the π_1, $n_{||}$, and σ_{CF} orbital regions with the metastable atom among several fluorobenzenes. It is found that the reactivity of the π_F, $n_{||}$, and σ_{CF} orbitals increase with the numbers of F atom substitutions, while that of the π_1 orbital does not. Attractive effects around the $n_{||}$ and σ_{CF} orbitals regions is basically enhanced with the increase of the substitution, whereas in some cases, a neighboring group effect becomes very important. On the other hand, the magnitude of an attractive interaction around the phenyl ring region decreases with the increment of the F atom substitution.

Acknowledgment. This work has been partially supported by a Grant in Aid for Scientific Research from the Japanese Ministry of Education, Science, and Culture. One of the authors (K.I) thanks the Japan Society for the Promotion of Science (JSPS) for a JSPS Research Fellowship.

References and Notes

(1) Penning, F. M. *Naturwissenschaften* **1927**, *15*, 818.
(2) For example, Siska, P. E. *Rev. Mod. Phys*. **1993**, *65*, 337, and references therein.
(3) Hotop, H.; Niehaus, A. *Z. Phys*. **1969**, *228*, 68.
(4) Ohno, K.; Mutoh, H.; Harada, Y. *J. Am. Chem. Soc*. **1983**, *105*, 4555.
(5) Ohno, K.; Matsumoto, S.; Harada, Y. *J. Chem. Phys*. **1984**, *81*, 4447.
(6) Ohno, K.; Yamakado, H.; Ogawa, T.; Yamata, T. *J. Chem. Phys*. **1996**, *105*, 7536.
(7) Tokue, I.; Sakai, Y.; Yamasaki, K. *J. Chem. Phys.* **1997**, *106*, 4491.
(8) Alberti, M.; Lucas, J. M.; Brunetti, B.; Pirani, F.; Stramaccia, M.; Rosi, M.; Vecchiocattivi, F. *J. Phys. Chem. A* **2000**, *104*, 1405.
(9) Yamato, M.; Ohoyama, H.; Kasai, T. *J. Phys. Chem. A* **2001**, *105*, 2967.
(10) Imura, K.; Kishimoto, N.; Ohno, K.. *J. Phys. Chem. A* **2001**, *105*, 6378.
(11) Imura, K.; Kishimoto, N.; Ohno, K.. *J. Phys. Chem. A* **2001**, *105*, 4189.
(12) Imura, K.; Kishimoto, N.; Ohno, K.. *J. Phys. Chem. A* **2001**, *105*, 6073.
(13) Takami, T.; Ohno, K. *J. Chem. Phys*. **1992**, *96*, 6523.
(14) Mitsuke, K.; Takami, T.; Ohno, K. *J. Chem. Phys*. **1989**, *91*, 1618.
(15) Ohno, K.; Takami, T.; Mitsuke, K.; Ishida, T. *J. Chem. Phys*. **1991**, *94*, 2675.
(16) Takami, T.; Mitsuke, K. Ohno, K. *J. Chem. Phys*. **1991**, *95*, 918.
(17) Gardner, J. L.; Samson, J. A. R. *J. Electron Spectrosc. Relat. Phenom*. **1976**, *8*, 469.
(18) Kimura, K.; Katsumata, S.; Achiba, Y.; Yamazaki, T.; Iwata, S. *Handbook of He I Photoelectron Spectra of Fundermental Organic Molecules*; Japan Scientific: Tokyo, 1981.
(19) Turner, D. W.; Baker, C.; Baker, A. D.; Brundle, C. R. *Molecular Photoelectron Spectroscopy*; Wiley: London, 1970.
(20) Yee, D. S. C.; Stewart, W. B.; Mcdowell, C. A.; Brion, C. E.*J. Electron Spectrosc. Relat. Phenom*. **1975**, *7*, 93.
(21) Hotop, H.; Hubler, G. *J. Electron Spectrosc. Relat. Phenom*. **1977**, *11*, 101.
(22) (a) Auerbach, D. J. *Atomic and Molecular Beam Methods*; Scoles, G., Ed.; Oxford University: New York, 1988; p 369. (b) Kishimoto, N.; Aizawa, J.; Yamakado, H.; Ohno, K. *J. Phys. Chem. A*. **1997**, *101*, 5038.
(23) Pauling, L.; *The Nature of Chemical Bond*; Cornell University: Ithaca, New York, 1960.
(24) Schlupf, J.; Weber, A. *J. Raman Spectry* **1973**, *1*, 103.
(25) Almenningen, A.; Hargittai, I.; Brunvoll, J.; Samdal, S. *J. Mol. Struct.* **1984**, *116*, 199.
(26) von Niessen, W.; Schirmer, J.; Cederbaum, L. S. *Comput. Phys. Rep*. **1984**, *1*, 57.
(27) (a) Zakrzewski, V. G.; Ortiz, J. V. *Int. J. Quantum Chem. Symp*. **1994**, *28*, 23. (b) Zakrzewski, V. G.; Ortiz, J. V. *Int. J. Quantum Chem.* **1995**, *53*, 583.
(28) Rothe, E. W.; Neynaber, R. H.; Trujillo, S. M. *J. Chem. Phys*. **1965**, *42*, 3310.
(29) Illenberger, E.; Niehaus, A. *Z. Phys. B* **1975**, *20*, 33.
(30) Parr, T.; Parr, D. M.; Martin, R. M. *J. Chem. Phys*. **1982**, *76*, 316.
(31) Hotop, H. *Radiat. Res*. **1974**, *59*, 379.
(32) Haberland, H.; Lee, Y. T.; Siska, P. E. *Adv. Chem. Phys*. **1981**, *45*, 487.
(33) Hotop, H.; Roth, T. E.; Ruf, M.-W.; Yencha, A. J. *Theor. Chem. Acc*. **1998**, *100*, 36.
(34) Yamakado, H.; Yamauchi, M.; Hoshino, S.; Ohno, K. *J. Phys. Chem*. **1995**, *99*, 55.
(35) Ohno, K.; Kishimoto, N.; Yamakado, H. *J. Phys. Chem.* **1995**, *99*, 9687.
(36) Yamakado, H.; Okamura, K.; Ohshimo, K.; Kishimoto, N.; Ohno, K. *Chem. Lett*. **1997**, 269.
(37) Kishimoto, N.; Ohshimo, K.; Ohno, K. *J. Electron Spectrosc. Relat. Phenom*. **1999**, *104*, 145.
(38) Kishimoto, N.; Osada, Y.; Ohno, K. *J. Phys. Chem. A* **2000**, *104*, 1393.
(39) Frisch, M. J.; Trucks, G. W.; Schlegel, H. B.; Scuseria, G. E.; Robb, M. A.; Cheeseman, J. R.; Zakrzewski, V. G.; Montgomery, Jr. J. A.; Stratmann, R. E.; Burant, J. C.; Dapprich, S.;. Millam, J. M; Daniels, A. D.; Kudin, K. N.; Strain, M. C.; Farkas, O.; Tomasi, J.; Barone, V.; Cossi, M.; Cammi, R.; Mennucci, B.; Pomelli, C.; Adamo, C.; Clifford, S.; Ochterski, J.; Petersson, G. A.; Ayala, P. Y.; Cui, Q.; Morokuma, K.; Malick, D. K.; Rabuck, A. D.; Raghavachari, K.; Foresman, J. B.; Cioslowski, J.; Ortiz, J. V.; Baboul, A. G.; Stefanov, B. B.; Liu, G.; Liashenko, A.; Piskorz, P.; Komaromi, I.; Gomperts, R.; Martin, R. L.; Fox, D. J.; Keith, T.; Al-Laham, M. A.; Peng, C. Y.; Nanayakkara, A.; Challacombe, M.; Gill, P. M. W.; Johnson, B.; Chen, W.; Wong, M. W.; Andres, J. L.; Gonzalez, C.; Head-Gordon, M.; Replogle, E. S.; Pople, J. A. Gaussian, Inc.: Pittsburgh, PA, 1998.
(40) Bieri, G.; Åsbrink, L.; von Niessen, W. *J. Electron Spectrosc. Relat. Phenom*. **1981**, *23*, 281.
(41) Palmer, M. H.; Moyes, W.; Spiers, M.; Ridyard, J. N. A. *J. Mol. Struct*. **1978**, *49*, 105.
(42) Turner, D. W.; Baker, C.; Baker, A. D.; Brundle, C. R. *Molecular Photoelectron Spectroscopy*; Wiley: London, 1970.
(43) Price, W. C.; Potts, A. W.; Gabliel A.; Williams, T. A. *Molecular Spectroscopy*; West, A. R., Ed.; Heyden: London, 1977; p 381.
(44) Price, W. C.; *Electron Spectroscopy*; Brundle, C. R., Baker, A. D. Eds.; Academic Press Inc.: London, 1977, *2*, p 152.
(45) Gilbert, R.; Sauvageau, P.; Sandorfy, C. *Chem. Phys. Lett*. **1972**, 17, 465.
(46) Duke, C. B.; Yip, K. L.; Ceasar, G. P.; Potts, A. W.; Streets, D. G. *J. Chem. Phys*. **1997**, *66*, 256.
(47) Potts, A. D.; Price, W. C.; Streets, D. G.; Williams, T. A. *J. Chem. Soc., Faraday Discuss*. **1972**, *54*, 168.
(48) Aoyama, M. Ph.D. Thesis, The University of Tokyo, 1989.
(49) Munakata, T.; Harada, Y.; Ohno, K.; Kuchitsu, K. *Chem. Phys. Lett*. **1981**, *84*, 6.
(50) Ohno, K.; Fujisawa, S.; Mutoh, H. Harada, Y. *J. Phys. Chem*. **1982**, *86*, 440.
(51) Harada, Y.; Ohno, K.; Mutoh, H. *J. Chem. Phys*. **1983**, *79*, 3251.
(52) Ohno, K.; Imai, K.; Matsumoto, S.; Harada, Y. *J. Phys. Chem*. **1983**, *87*, 4346.